Hindawi Publishing Corporation
EURASIP Journal on Wireless Communications and Networking
Volume 2008, Article ID 513971, 6 pages
doi:10.1155/2008/513971

Research Article

Mapping Rearrangement for Parallel Concatenated Trellis Coded Modulation

Mustapha Benjillali and Leszek Szczecinski

Institut National de la Recherche Scientifique (INRS), Centre Énergie Matériaux et Télécommunications (EMT), Montreal, QC, Canada H5A 1K6

Correspondence should be addressed to Mustapha Benjillali, benjillali@ieee.org

Received 29 May 2008; Revised 23 October 2008; Accepted 12 December 2008

Recommended by Wolfgang Gerstacker

Mapping rearrangement (MaRe) for the hybrid ARQ (HARQ) based on the parallel concatenated trellis coded modulation (PCTCM) is analyzed. We demonstrate that the performance of the PCTCM receiver is intrinsically limited by the MaRe design and we propose a new mapping scheme to fit the structure of PCTCM transceivers. Depending on the HARQ scenarios, the proposed scheme offers gains between 0.1 and 2.4 dB when compared with known MaRe schemes.

1. INTRODUCTION

In this paper, we propose a mapping rearrangement (MaRe) scheme suitable for the parallel concatenated trellis coded modulation (PCTCM) in the automatic repeat request (ARQ) context. This retransmission mechanism increases the reliability of the communication link and handles the retransmissions of erroneous data packets. It is commonly combined with channel coding and called *hybrid ARQ* (HARQ). Here, we analyze HARQ schemes where the binary contents of all transmissions are identical and the difference between the retransmissions resides only in the bits-to-symbols mappings. When appropriately designed, such a *mapping rearrangement* (MaRe) (also known as *mapping diversity*) may offer important performance gains.

MaRe designs were initially proposed in [1, 2] and recently the authors of [3] presented an MaRe scheme—which we will refer to as "MBER" in this paper—that minimizes the uncoded bit error rate (BER). Similar results—from the performance point of view—based on the maximization of the minimum-squared Euclidean distance (MSED) were also obtained in [4]. Finally, a particular form of MaRe—also known as the constellation rearrangement (CoRe)—was already applied in the high-speed downlink packet access (HSDPA) [5, 6].

The capacity-based analysis of HARQ with MaRe presented in [7, 8] revealed that the constrained coded modulation (CM) capacity [9] (i.e., the average mutual information between the channel outcome and the transmitted modulated symbol) of the optimized MBER mapping is the largest among other known MaRe schemes (such as CoRe). But when the bit-interleaved coded modulation (BICM) capacity [9] is used for comparison, it was demonstrated in [8] that for certain nominal spectral efficiencies, MBER may turn out to be useless and may even be outperformed by transmissions with a simple repetition, that is, without any form of MaRe. These conclusions were confirmed by simulation results of BICM systems [8, 10].

The failure of the simple and flexible coded modulation schemes such as BICM to adequatly exploit the advantages of the optimized MBER design over the heuristic CoRe provides us with the motivation to revisit some of the interesting "spectrally efficient" CM schemes, that is, which perform within 1-2 dB of the capacity limits. Analyzing various CM schemes proposed in the literature, for example, [11–13], we choose the parallel concatenated trellis coded modulation (PCTCM) [13] which seems to offer the best performance among the studied coded-modulation schemes.

The need to take into account the coded modulation scheme during the MaRe design becomes apparent when we

realize that the existing CM schemes are optimized for the first transmission but are not necessarily optimal for the subsequent retransmissions. In particular, PCTCM is designed assuming the independence of the observations related to its constituent encoders. This assumption, while true in the first transmission, does not hold in the retransmissions. The contribution of this paper is twofold: we propose a simple design method that makes MaRe scheme fit the PCTCM transceiver, and we explain what are the theoretical limits of the PCTCM receivers.

We propose to change the design of the mapping during the retransmissions to take into account the operational principles of PCTCM receivers. The mapping that results could be seen as a new MSED mapping rearrangement and we will refer to this second proposed scheme as *MSED*. Although such a joint (coding-mapping) design slightly decreases the theoretical capacity limits when compared to MBER mapping, the practical performance of the resulting MaRe scheme is significantly better while the complexity of the receiver is not altered.

2. SYSTEM MODEL

We analyze the system whose baseband model is shown in Figure 1. The coded modulation scheme we adopt here was proposed (for one transmission) in [13] to achieve the nominal spectral efficiency of 2 bits per channel use (2 bpc) using 16-ary quadrature amplitude modulation (16-QAM). Note that different spectral efficiencies may be obtained by changing the code rate and/or the modulation order. However, working with the spectral efficiency of 2 bpc does not only allow us to focus on a specific case, but also is a particularly relevant comparison setup. Indeed, for higher spectral efficiencies, MBER outperforms CoRe in terms of capacity and practical performance even when suboptimal BICM is used [8]. For spectral efficiencies lower than 2 bpc, it would be more practical to change the modulation order rather than lowering the coding rate. (Note that from the implementation standpoint, and since the detection complexity increases with the modulation order, one would opt for 4-QAM rather than 16-QAM if the target spectral efficiency is less than 2 bpc). Thus, 2 bpc is a "breakpoint" spectral efficiency suitable to demonstrate the effectiveness of a CM scheme (such as the PCTCM we choose).

In the considered system, a sequence of quaternary (i.e., defined by 2 bits) information symbols $\mathbf{b}(n)$—where n denotes the discrete transmission time—and its interleaved version are encoded by two rate-2/3 recursive 16-states convolutional encoders ($\mathcal{C}_{\mathcal{R}}$ and $\mathcal{C}_{\mathcal{I}}$) with forward and backward generators given, respectively, by $\{35,27\}_8$ and $\{23\}_8$. The interleaving is performed at the bit-level [13] using two S-random interleavers of length 2048 bits, with $S = 40$ and $S = 32$. After the appropriate puncturing [13], the obtained sequences of quaternary symbols $\mathbf{c}_{\mathcal{I}}(n)$ and $\mathbf{c}_{\mathcal{R}}(n)$ are merged into 16-ary symbols $\mathbf{c}(n) = [\mathbf{c}_{\mathcal{I}}(n), \mathbf{c}_{\mathcal{R}}(n)]$. We adopt the indexing $\mathcal{I}$ and $\mathcal{R}$ in accordance with the original design of [13] where the symbols $\mathbf{c}_{\mathcal{I}}(n)$ and $\mathbf{c}_{\mathcal{R}}(n)$ were mapped, respectively, into imaginary ($\mathcal{I}$) and real ($\mathcal{R}$) parts of the symbols.

While the coding is unaltered throughout the retransmissions (i.e., the same sequence of coded words $\mathbf{c}(n)$ of length m in $\mathcal{B} = \{0,1\}^m$ is sent), the operator $\mu_t[\cdot] : \mathcal{B} \to \mathcal{X}$ that maps $\mathbf{c}(n)$ onto symbols taken from a normalized 16-QAM constellation $\mathcal{X}$ (i.e., $(1/2^m)\sum_{\mathbf{c}\in\mathcal{B}}|\mu_t[\mathbf{c}]|^2 = 1$ and $\sum_{\mathbf{c}\in\mathcal{B}}\mu_t[\mathbf{c}] = 0$) is changing with $t = 1,\ldots,T$ (hence the name, *mapping rearrangement*), where T is the maximum allowed number of transmissions. We focus here on unfaded channels (as done, e.g., in [3, 14]) so the received signal in the tth transmission is given by $r_t(n) = x_t(n) + \eta_t(n)$, where $x_t(n) = \mu_t[\mathbf{c}(n)]$, $\eta_t(n)$ is a complex additive white Gaussian noise (AWGN) with variance $1/\gamma$, and γ is the average signal-to-noise ratio (SNR).

At the receiver, two decoders $\mathrm{APP}_{\mathcal{R}}\{\cdot\}$ and $\mathrm{APP}_{\mathcal{I}}\{\cdot\}$ decode the transmitted data in a "turbo" manner, that is, by exchanging reliability metrics they calculate for the information symbols in the form of extrinsic probabilities. Each decoder uses the channel-related metrics and a priori metrics obtained from the complementary decoder to produce the extrinsic reliability metrics $L_{\mathcal{R}}(\mathbf{b}(n))$ and $L_{\mathcal{I}}(\mathbf{b}(n))$ for the information symbols $\mathbf{b}(n)$:

$$\begin{aligned} &L_{\mathcal{R}}(\mathbf{b}(n)) \\ &\quad = \mathrm{APP}_{\mathcal{R}}\left[\ln\left\{\sum_{\mathbf{c}_{\mathcal{I}}\in\{0,1\}^2} \mathrm{p}(\mathbf{r}(n) \mid \mathbf{c}_{\mathcal{R}}, \mathbf{c}_{\mathcal{I}})\right\}, L^{\mathrm{a}}_{\mathcal{R}}(\mathbf{b}(n))\right] \\ &\qquad - L^{\mathrm{a}}_{\mathcal{R}}(\mathbf{b}(n)), \\ &L_{\mathcal{I}}(\mathbf{b}(n)) \\ &\quad = \mathrm{APP}_{\mathcal{I}}\left[\ln\left\{\sum_{\mathbf{c}_{\mathcal{R}}\in\{0,1\}^2} \mathrm{p}(\mathbf{r}(n) \mid \mathbf{c}_{\mathcal{R}}, \mathbf{c}_{\mathcal{I}})\right\}, L^{\mathrm{a}}_{\mathcal{I}}(\mathbf{b}(n))\right] \\ &\qquad - L^{\mathrm{a}}_{\mathcal{I}}(\mathbf{b}(n)), \end{aligned} \tag{1}$$

where the a priori metrics $L^{\mathrm{a}}_{\mathcal{R}}$ and $L^{\mathrm{a}}_{\mathcal{I}}$ are (de)interleaved versions of the metrics $L_{\mathcal{I}}$ and $L_{\mathcal{R}}$, respectively. The algorithm $\mathrm{APP}_{\mathcal{R}/\mathcal{I}}[\nu(n), L^{\mathrm{a}}_{\mathcal{R}/\mathcal{I}}(\mathbf{b}(n))]$ uses the *sequences* of the channel-related metrics $\nu(n)$ calculated from the channel outcomes collected in the vector $\mathbf{r} = [r_1(n),\ldots,r_T(n)]$, and $\mathrm{p}(\mathbf{r}|\mathbf{c}) = (\gamma^T/(2\pi)^T)\exp(-\gamma\|\mathbf{r} - \boldsymbol{\mu}[\mathbf{c}]\|^2)$, where $\boldsymbol{\mu}[\mathbf{c}] = [\mu_1[\mathbf{c}],\ldots,\mu_T[\mathbf{c}]]$. The decoders implement—in a computationally efficient manner—the maximum a posteriori (MAP) algorithm described in detail in [11].

We observe that, in general, the marginalization over the real/imaginary parts is required to calculate the decoding metrics (as indicated by the sums within the logarithm in (1)). However, as already mentioned, during the first transmission ($t = 1$), the codewords $\mathbf{c}_{\mathcal{R}}(n)$ and $\mathbf{c}_{\mathcal{I}}(n)$ are mapped independently into the real and imaginary parts of the symbol $x_1(n)$. When this is also the case for subsequent transmissions, we can write

$$\boldsymbol{\mu}[\mathbf{c}_{\mathcal{R}}(n), \mathbf{c}_{\mathcal{I}}(n)] = \underline{\boldsymbol{\mu}}[\mathbf{c}_{\mathcal{R}}(n)] + \jmath\cdot\underline{\boldsymbol{\mu}}[\mathbf{c}_{\mathcal{I}}(n)], \tag{2}$$

where $\underline{\boldsymbol{\mu}}[\mathbf{c}] = [\underline{\mu}_1[\mathbf{c}],\ldots,\underline{\mu}_T[\mathbf{c}]]$ and $\underline{\mu}_t[\mathbf{c}]$ is the tth transmission mapping of the quaternary codeword $\mathbf{v}$ into the

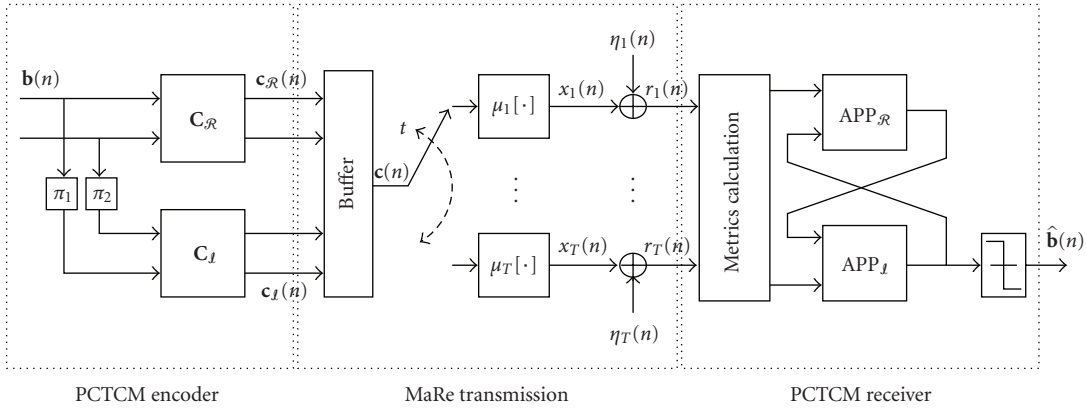

Figure 1: Baseband model of MaRe transmission with PCTCM tranceivers. In the tth transmission, the modulation is based on the mapping $\mu_t[\cdot]$.

real or imaginary part of the symbol. Then, (1) immediately simplify to

$$\begin{aligned} &L_{\mathcal{R}}(\mathbf{b}(n)) \\ &\quad = \mathrm{APP}_{\mathcal{R}}\left[-\gamma\left\|\mathbf{r}_{\mathcal{R}}(n) - \underline{\boldsymbol{\mu}}[\mathbf{c}_{\mathcal{R}}]\right\|^2, L^{\mathrm{a}}_{\mathcal{R}}(\mathbf{b}(n))\right] - L^{\mathrm{a}}_{\mathcal{R}}(\mathbf{b}(n)), \\ &L_{\mathcal{I}}(\mathbf{b}(n)) \\ &\quad = \mathrm{APP}_{\mathcal{I}}\left[-\gamma\left\|\mathbf{r}_{\mathcal{I}}(n) - \underline{\boldsymbol{\mu}}[\mathbf{c}_{\mathcal{I}}]\right\|^2, L^{\mathrm{a}}_{\mathcal{I}}(\mathbf{b}(n))\right] - L^{\mathrm{a}}_{\mathcal{I}}(\mathbf{b}(n)). \end{aligned} \tag{3}$$

3. MAPPING REARRANGEMENT DESIGN FOR THE PCTCM TRANSCEIVER

If multiple transmissions are considered, the property (2) is not always preserved. Besides the mapping rearrangement we propose in Section 3.1, two mappings taken from the literature are considered in this work. CoRe mapping is obtained through bits swapping and/or negation within the codeword [5, 6, 15] and aims to "equalize" the bits reliability in different transmissions. The swapping is always done within the two bits related to the real or imaginary part of the symbol (here, the first and the third or the second and the fourth bits, resp., as shown in Figure 2(a)), so (2) holds for $T = 2, 3, 4$ and the metrics may be calculated as shown in (3). On the other hand, considering the MBER mapping taken from [3] and shown in Figure 2(b), it is easy to verify that the real and imaginary components are not mapped independently. For example, when $t = 2$, the second and the fourth bits are not the same for the symbols with the same imaginary value. Consequently, we cannot use (3), but rather (1) should be applied.

As we will see through the numerical examples, this will produce a poor performance when MBER mapping is used, and this performance degradation motivates us to redesign a suitable mapping rearrangement scheme for PCTCM receivers. Also, in order to explain these results, we will look in Section 3.2 at the theoretical limits of the PCTCM transceiver used with MaRe.

3.1. New MaRe design

We now propose a new MaRe scheme that maintains the constraint of separability between the real and imaginary parts of the modulated symbols as shown in (2).

Since we consider identical mappings for both real and imaginary branches, we only need to design the mappings $\underline{\mu}_t[\cdot]$ for every transmission $t = 1, \ldots, T$. To this end, we propose to maximize the minimum squared Euclidean distance (MSED) between the subsequent constellation points as done in [4]. Thus, our design could be seen as a new MSED mapping rearrangement scheme. The search for the optimal MSED mapping is a tree-search procedure [1, 4], starting with the mapping $\underline{\mu}_t[\cdot]$ having the highest MSED value at the tth transmission, and looking for the best candidate $\underline{\mu}_{t+1}[\cdot]$ for the subsequent transmission $t + 1$, until the tth mapping is found. The details of the search are not relevant to the main contribution of the paper, but we refer the interested reader to [1], where simple examples are shown.

Since the optimization space is not very large in our case (for quaternary symbols, the upper bound on the number of existing mappings $\underline{\mu}_t[\cdot]$ is given by $4! = 24$), the search for the new MSED mapping may be done exhaustively, without resorting to integer programing techniques applied, for example, in [3, 4]. The obtained results are shown in Figure 3.

3.2. PCTCM capacity limits

The metrics are calculated for the quaternary symbols $\mathbf{c}_{\mathcal{R}}(n)$ and $\mathbf{c}_{\mathcal{I}}(n)$ using the channel outcome that is affected by the 16-ary symbols $[\mathbf{c}_{\mathcal{R}}(n), \mathbf{c}_{\mathcal{I}}(n)]$. The effect of the symbol $\mathbf{c}_{\mathcal{I}}(n)$ on the metric $L_{\mathcal{R}}(\mathbf{b}(n))$ (and vice versa) may be easily understood via analogy with BICM [9], where the metrics calculated at the bit-level do not convey the same information as the probabilities calculated for the sent symbols. This leads to a suboptimal detection and consequently the BICM capacity is always smaller than the CM capacity.

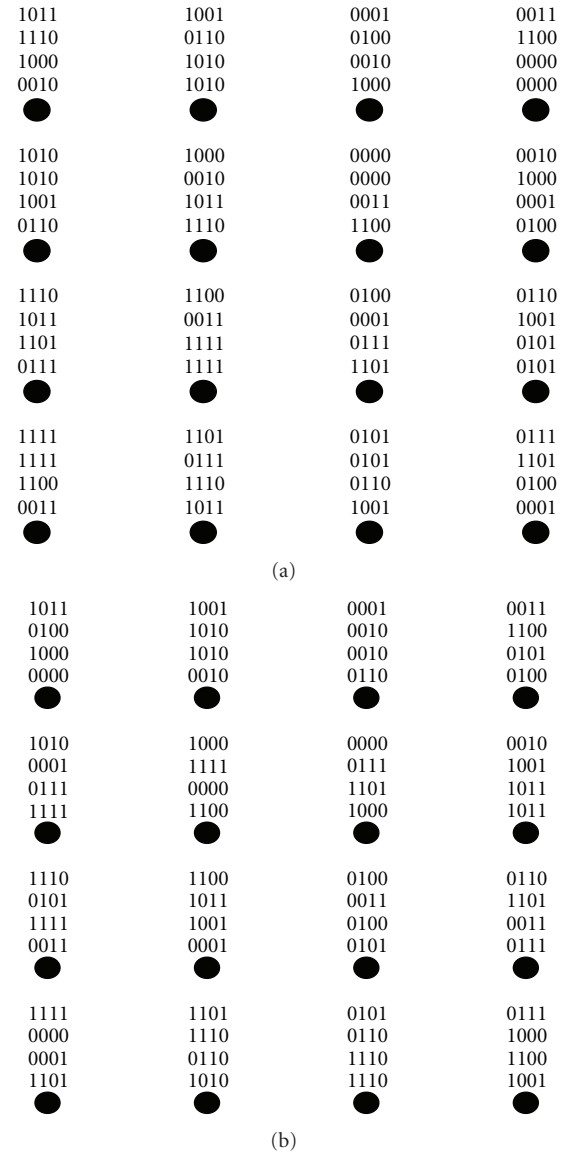

Figure 2: The 16-QAM mappings used during the study: (a) CoRe [6, 15] and (b) MBER [3]. The filled circles represent the constellation points. The labels are read from top to bottom for transmissions $t = 1, \ldots, 4$. The upper labels correspond to the mapping $\mu_1[\cdot]$ which is always gray, that is, the first and the third bits are mapped into the real part of the symbols, while the second and the fourth bits into the imaginary ones.

Generalizing the results of [9, 16], we propose to calculate what we call herein the *PCTCM capacity*, that is, the average mutual information between quaternary symbols $\mathbf{c}_{\mathcal{R}}(\mathbf{b}(n))$ and $\mathbf{c}_{\mathcal{I}}(\mathbf{b}(n))$ and the inputs to the corresponding APP decoders shown in (1).

To keep the considerations relatively general, we consider a scheme, where the channel input codeword $\mathbf{c} \in \mathcal{B}$ is split into K subcodewords $\mathbf{c}_k$ as $\mathbf{c} = [\mathbf{c}_1, \ldots, \mathbf{c}_K]$, and where the reliability metrics are obtained for each $\mathbf{c}_k$ using the channel outcome $\mathbf{r}$ affected by $\mathbf{c}$; in our case $K = 2$. The transmission channel may then be seen as a concatenation of

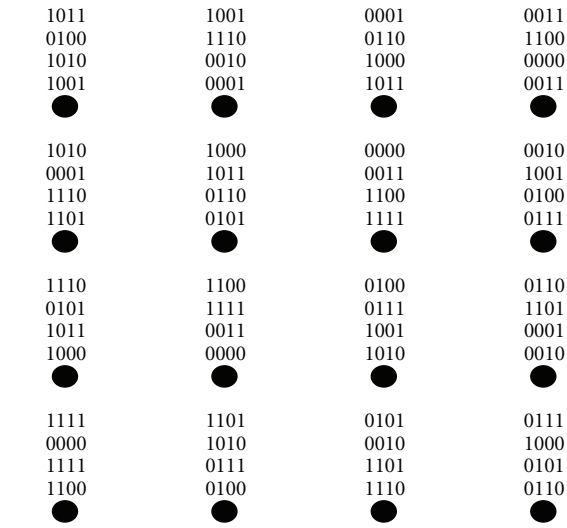

Figure 3: Proposed MSED mappings. The labeling convention from Figure 2 is followed.

K parallel channels, and its capacity results from the sum of all subchannels mutual information [9] which can be derived as

$$\begin{aligned}\overline{C} &= \sum_{k=1}^{K} I(\mathbf{c}_k, \mathbf{r}) \\ &= \sum_{k=1}^{K} \left(\frac{m}{K} - \mathrm{E}_{\mathbf{c}_k,\mathbf{r}} \left[\log_2 \frac{\sum_{\mathbf{c}\in\mathcal{B}} \mathrm{p}(\mathbf{r} \mid \mathbf{c})}{\sum_{\mathbf{c}\in\mathcal{B}_{k,\mathbf{c}_k}} \mathrm{p}(\mathbf{r} \mid \mathbf{c})} \right] \right) \\ &= m - \sum_{k=1}^{K} \mathrm{E}_{\mathbf{c}_k,\mathbf{r}} \left[\log_2 \sum_{\mathbf{c}\in\mathcal{B}} \mathrm{p}(\mathbf{r} \mid \mathbf{c}) \right] \\ &\quad + \sum_{k=1}^{K} \mathrm{E}_{\mathbf{c}_k,\mathbf{r}} \left[\log_2 \sum_{\mathbf{c}\in\mathcal{B}_{k,\mathbf{c}_k}} \mathrm{p}(\mathbf{r} \mid \mathbf{c}) \right],\end{aligned} \tag{4}$$

where $I(\mathbf{c}_k, \mathbf{r})$ is the mutual information between the channel outcome $\mathbf{r}$ and the subcodeword $\mathbf{c}_k$, and $\mathcal{B}_{k,\mathbf{v}}$ is the set of $\mathbf{c} \in \mathcal{B}$ such that the kth subcodeword of $\mathbf{c}$ is $\mathbf{v}$.

After simple transformations, we obtain the expression of PCTCM capacity that may be calculated using Monte Carlo technique or via multidimensional integration as

$$\begin{aligned}\overline{C} &= m - \frac{K}{2^m} \sum_{\mathbf{c}\in\mathcal{B}} \mathrm{E}_{\boldsymbol{\eta}} \left[\log_2 \sum_{\mathbf{v}\in\mathcal{B}} \mathrm{p}(\boldsymbol{\mu}[\mathbf{v}] + \boldsymbol{\eta} \mid \mathbf{c}) \right] \\ &\quad + \frac{1}{2^m} \sum_{\mathbf{c}\in\mathcal{B}} \mathrm{E}_{\boldsymbol{\eta}} \left[\sum_{k=1}^{K} \log_2 \sum_{\mathbf{v}\in\mathcal{B}_{k,\mathbf{c}_k}} \mathrm{p}(\boldsymbol{\mu}[\mathbf{v}] + \boldsymbol{\eta} \mid \mathbf{c}) \right].\end{aligned} \tag{5}$$

This solution generalizes the expressions known from [9]: setting $K = m$ gives the BICM capacity, while for $K = 1$, the CM capacity is obtained.

Evaluating (5) as a function of γ, we can find the SNR for which the target spectral efficiency (here 2 bpc) is theoretically attainable. The values of these SNR limits are presented in Table 1, where we contrast them with

Table 1: Minimum SNR required to attain the spectral efficiency of 2 bpc for $T = 2, 3, 4$ transmissions.

	$T = 2$	$T = 3$	$T = 4$
CoRe (CM)	0.6 dB	−1.7 dB	−3.1 dB
MBER (CM)	0.1 dB	−2.1 dB	−3.4 dB
MBER (PCTCM)	1.7 dB	−0.6 dB	−2.2 dB
New MSED (PCTCM)	0.2 dB	−1.8 dB	−3.2 dB

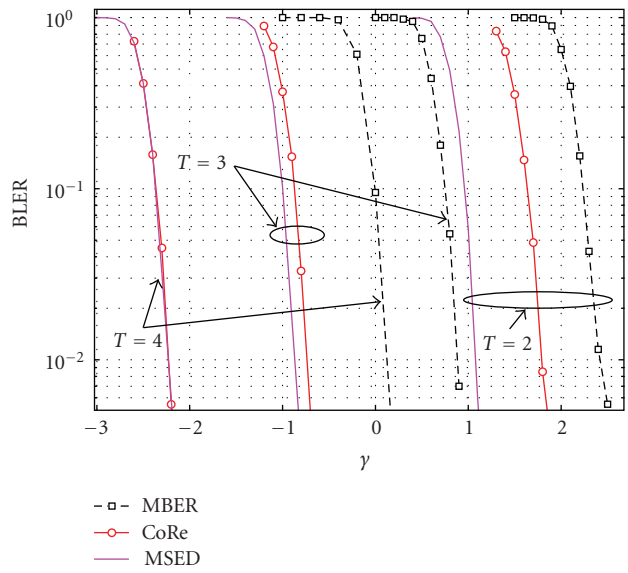

Figure 4: BLER obtained using the analyzed mappings for $T = 2, 3$, and 4 transmissions. The results labeled as MBER, CoRe, and MSED are obtained for the respective mappings with a PCTCM receiver.

the CM capacity results obtained in [8] for CoRe and MBER. We observe that using the metrics obtained for the quaternary symbols (PCTCM capacity with MBER) leads to a 1.7–1.2 dB loss when compared to using 16-ary symbols metrics (CM capacity with MBER). This large capacity gap places the PCTCM capacity with MBER 1 dB below the CM capacity with CoRe mapping. Thus, although MBER mapping provides theoretically interesting capacity limits, choosing PCTCM for the first transmission impairs the effectiveness of the retransmissions.

On the other hand, by calculating the capacity limits for the proposed MSED mapping (cf., Table 1), we note an interesting pragmatic tradeoff: theoretical capacity limits of our new MSED mapping are slightly lower (by 0.1-0.2 dB) with respect to CM capacity of MBER, but the performance of the practical coding scheme is improved (as will be shown by simulation results in Section 4).

4. SIMULATION RESULTS

Simulation results obtained for CoRe and for the mappings using the "conventional" PCTCM receiver are presented in Figure 4. We compare the capacity limits with the SNR required to attain a block error rate (BLER) of 0.01, that is, where the throughput attains 99% of the nominal spectral efficiency [17]. The performance obtained by CoRe is clearly superior than the one corresponding to the MBER mapping. This confirms that comparing CM and PCTCM capacities provides a valuable insight into the difference of performance that may be expected from the practical coding schemes.

The proposed MSED mapping performs better than CoRe for $T = 2, 3$. It provides practically the same performance for $T = 4$, and the reason is that PCTCM encoders are optimized for Gray-mapped constellations. While the Gray mapping property is preserved in CoRe for all T transmissions, it holds only for $t = 1$ in the optimized MSED mapping. Therefore, since CoRe is adjusted to approach the capacity limits, for $T = 4$ where CoRe and MSED capacities are close to each other, the performances of PCTCM receivers with both MSED and CoRe schemes become comparable. However, note that the good performance of the new MSED during the first HARQ transmissions could make a fourth transmission even unnecessary and the comparison with CoRe would not even take place for $T = 4$.

5. CONCLUSION

In this work, we analyzed the applicability of some mapping rearrangement schemes suitable for parallel concatenated trellis coded modulation for retransmissions in the hybrid ARQ context. We showed that the performance of the conventional PCTCM is severely limited with known mappings from the literature. We identified these limitations and proposed to redesign the mapping in order to adjust its properties to the structure of PCTCM receivers. We demonstrated that the proposed mapping offers an interesting tradeoff: it decreases the theoretical limits (in terms of capacity) in order to improve the performance of the practical coding scheme (in terms of throughput). These results indicate that to guarantee the gains of the mapping rearrangement, the solution should be sought in the mapping/coding codesign.

ACKNOWLEDGMENTS

This work was supported by NSERC, Canada, (under Alexander Graham Bell Canada Graduate Scholarship and research Grant 249704-07). Part of this work was presented at the IEEE International Conference on Communications 2008 (ICC '08), 19–23 May 2008, Beijing, China.

REFERENCES

[1] J. J. Metzner, "Improved sequential signaling and decision techniques for nonbinary block codes," *IEEE Transactions on Communications*, vol. 25, no. 5, pp. 561–563, 1977.

[2] G. Benelli, "A new method for the integration of modulation and channel coding in an ARQ protocol," *IEEE Transactions on Communications*, vol. 40, no. 10, pp. 1594–1606, 1992.

[3] H. Samra, Z. Ding, and P. M. Hahn, "Symbol mapping diversity design for multiple packet transmissions," *IEEE Transactions on Communications*, vol. 53, no. 5, pp. 810–817, 2005.

[4] L. Szczecinski and M. Bacic, "Constellations design for multiple transmissions: maximizing the minimum squared

Euclidean distance," in *Proceedings of IEEE Wireless Communications and Networking Conference (WCNC '05)*, vol. 2, pp. 1066–1071, New Orleans, La, USA, March 2005.

[5] 3GPP, "Universal mobile telecommunications system (UMTS); multiplexing and channel coding (FDD)," Tech. Rep. TS 25.212, ETSI, Cedex, France, December 2003.

[6] C. Wengerter, A. G. E. von Elbwart, E. Seidel, G. Velev, and M. P. Schmitt, "Advanced hybrid ARQ technique employing a signal constellation rearrangement," in *Proceedings of the 56th IEEE Vehicular Technology Conference (VTC '02)*, vol. 4, pp. 2002–2006, Vancouver, Canada, September 2002.

[7] L. Szczecinski, F.-K. Diop, M. Benjillali, A. Ceron, and R. Feick, "BICM in HARQ with mapping rearrangement: capacity and performance of practical schemes," in *Proceedings of the 50th Annual IEEE Global Telecommunications Conference (GLOBECOM '07)*, pp. 1410–1415, Washington, DC, USA, November 2007.

[8] L. Szczecinski, F.-K. Diop, and M. Benjillali, "On the performance of BICM with mapping diversity in hybrid ARQ," *Wireless Communications and Mobile Computing*, vol. 8, no. 7, pp. 963–972, 2008.

[9] G. Caire, G. Taricco, and E. Biglieri, "Bit-interleaved coded modulation," *IEEE Transactions on Information Theory*, vol. 44, no. 3, pp. 927–946, 1998.

[10] X. Li and J. A. Ritcey, "Bit-interleaved coded modulation with iterative decoding," *IEEE Communications Letters*, vol. 1, no. 6, pp. 169–171, 1997.

[11] P. Robertson and T. Wörz, "Bandwidth-efficient turbo trellis-coded modulation using punctured component codes," *IEEE Journal on Selected Areas in Communications*, vol. 16, no. 2, pp. 206–218, 1998.

[12] S. Y. Le Goff, A. Glavieux, and C. Berrou, "Turbo-codes and high spectral efficiency modulation," in *Proceedings of IEEE International Conference on Communications (ICC '94)*, vol. 2, pp. 645–649, New Orleans, La, USA, May 1994.

[13] S. Benedetto, D. Divsalar, G. Montorsi, and F. Pollara, "Parallel concatenated trellis coded modulation," in *Proceedings of IEEE International Conference on Communications (ICC '96)*, vol. 2, pp. 974–978, Dallas, Tex, USA, June 1996.

[14] Panasonic, "Enhanced HARQ method with signal constellation rearregement," Tech. Rep. TSG RAN WG1, Cedex, France, 3GPP, March 2001.

[15] K. Miyoshi, A. Matsumoto, C. Wengerter, M. Kasapidis, M. Uesugi, and O. Kato, "Constellation rearrangement and spreading code rearrangement for hybrid ARQ in MC-CDMA," in *Proceedings of the 5th International Symposium on Wireless Personal Multimedia Communications (WPMC '02)*, vol. 2, pp. 668–672, Honolulu, Hawaii, USA, October 2002.

[16] S. Y. Le Goff, "Signal constellations for bit-interleaved coded modulation," *IEEE Transactions on Information Theory*, vol. 49, no. 1, pp. 307–313, 2003.

[17] C. Schlegel and L. Peréz, "On error bounds and turbo-codes," *IEEE Communications Letters*, vol. 3, no. 7, pp. 205–207, 1999.